Submitted to Journal of Chemical Physics

LBL-4593
Preprint c.1

PENNING IONIZATION OF $He(2^3S)+Ar$

Z. F. Wang, Albert P. Hickman, Kosuke Shobatake, and Y. T. Lee

January 1976

Prepared for the U. S. Energy Research and Development Administration under Contract W-7405-ENG-48

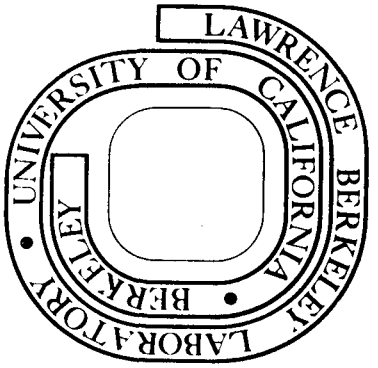

DISCLAIMER

PENNING IONIZATION OF $He(2^3S)+Ar^{\dagger}$

Z.F. Wang, Albert P. Hickman, Kosuke Shobatake[‡] and Y. T. Lee

Materials and Molecular Research Division
and
Department of Chemistry

Lawrence Berkeley Laboratory
University of California
Berkeley, California 94720

January 1976

ABSTRACT

A new measurement of the differential cross sections for $He(2^3S)+Ar$ has been carried out at 65 and 132 meV. A potential V_0-iV_i is found which fits our data as well as the total ionization cross section results of Illenberger and Niehaus. Some sources of uncertainties inherent in our analysis are discussed. The first order semiclassical approximation, which has been employed by several groups, is critically examined. A guideline is proposed to define the region within which this approach can be safely adopted.

INTRODUCTION

The phenomenon of Penning ionization is currently commanding a great deal of research effort. Much data has been compiled for systems ranging from the rare gas atoms to simple molecules. The interaction between $He(2^3S)$+Ar has established itself as one of the prototype systems for this important physical process. The reader is referred to ref. 1 for a recent review in this area.

Total and differential cross section measurements, Penning electron energy distributions, as well as theoretical calculations have all been carried out for $He(2^3S)$+Ar.[2-5,10] Essentially, three quantities are needed to give a complete description of this inelastic collision process, they are (a) V_0, the interaction potential between the metastable helium and ground state argon, (b) V_i, the imaginary part of the potential which accounts for the ionization, and (c) the ionic potential, V_+, for $HeAr^+$. All three are susceptible to experimental investigation: the first two from total and differential cross section data, and the third, given a particular V_0 and V_i, can be inferred from the energy distribution of Penning electrons and the ratio of Penning to associative ionization. This paper is primarily addressed to V_0 and V_i. It is fair to remark that, despite much determination, none of the candidates for V_0-iV_i advanced thus far concurs with all the available information. For example, Illenberger and Niehaus[2] as well as Pesnelle, Watel and Manus[3] have, using the potential proposed by Olson, derived a V_i which yielded fairly good agreement with their measured energy dependence of total ionization cross section. However, the differential cross section calculated from Olson's V_0 and their respective V_i failed to be compatible with experimental results. It should be pointed out that the very recent calculations by Hickman and Morgner[11] have resulted in a Morse form for V_0. The well for this potential was believed to be accurate, but there were some uncertainties as to the steepness of the wall.

Our group has previously performed differential cross section measurement for this system.[4] $He(2^3S)$+Ar is in many ways very suited to beam studies as ionization is known to take place at very small impact

parameters. Thus only the large angle region of the differential cross section is affected, enabling one to extract in the conventional manner the real part of the potential around and outside of the well region from the measurements at small angles. Having obtained the real part, one proceeds to represent the imaginary part of the potential by a suitable functional form whose parameters are then adjusted to fit the large angle data.

The experimental results we reported earlier however had sizable uncertainties at large angles. They also showed an anomalous dip at around 60° (lab. frame), which among other difficulties, defied a good theoretical explanation. For this reason, we have undertaken the same measurement again, this time exercising greater perseverance in cutting down the uncertainties. To our great satisfaction, the dip went away. We have scanned the differential cross section at two collision energies, 65 meV and 132 meV. The potential we propose this time reproduces very well the total ionization cross section data of Illenberger and Niehaus,[2] and is also substantially in harmony with the recent more detailed study by Haberland and Schmidt.[2]

In our analysis of the data, we used a semiclassical approximation to calculate the real and imaginary parts of the phase shifts. While this approach was adopted in most previously reported works, we recognize that its validity rests on the assumption that the imaginary part of the potential V_i acts as a perturbation on the real part, V_0. That is $V_i \ll V_0$. It is therefore important to determine the maximum bound for V_i below which this approximation holds. To this end, we have varied our best fit V_i by a few orders of magnitude to observe changes in the calculated differential cross sections. The corresponding quantum mechanical calculations were also performed for comparison.

EXPERIMENTAL

The molecular beam apparatus used in our experiment has been described elsewhere.[4]

The metastable He is produced by crossing a supersonic He beam with an electron beam perpendicular to it. The electrons were emitted

by a tungsten filament, and accelerated through a potential of 250 V. The resulting emission current was typically 60 mA.

Since the electron excitation generated both He[2^1S] and He(2^3S), a helical pyrex He resonance lamp was used to quench away the He(^{1}S). The lamp was cooled with running water, and was operated at 2000 V. After collimation through a set of defining slits, the He(2^3S) beam, with about 1° FWHM, registered an intensity of ~10^{10} atoms/sec as collected by a Be-Cu Faraday cup. The velocity spread of the metastable beam was 6%-8% FWHM.

Likewise, the Ar beam was produced by a supersonic expansion at room temperature. Its FWHM angular and velocity spread were 2° and 6%-8% respectively.

The collision energy was varied by changing the nozzle temperature of the He beam. The pressure behind the nozzle for each reactant gas was adjusted to optimize the signal to noise at 20° (lab). The counting time for each angle was chosen to give maximal statistical reproducibility of the signal, it was generally set at 45 sec.

The data reported here are the average of 8 scans at 65 meV and 3 scans at 132 meV.

ANALYSIS

The measured differential cross sections for He(2^3S)+Ar at 65 meV and 132 meV are shown in Fig. 1. A MMSV potential was used to fit the data:

$$f(x) = \exp[-2\beta_1(x-1)] - 2\exp[-\beta_1(x-1)] \qquad x_1 < x \leq 1$$
$$f(x) = \exp[-2\beta_2(x-1)] - 2\exp[-\beta_2(x-1)] \qquad 1 < x \leq x_2$$
$$f(x) = b_1 + (x-x_2)\{b_2 + (x-x_3)[b_3 + (x-x_2)\,b_4]\} \qquad x_2 < x \leq x_3$$
$$\rho(x) = -c_6 x^{-6} - c_8 x^{-8} \qquad x_3 < x \leq \infty$$

where

$$f(x) = \frac{V(r)}{\epsilon}\ ;\quad x = \frac{r}{r_m}\ ;\quad c_n = \frac{C_n}{\epsilon\, r_m^n}\ . \qquad (1)$$

The potential parameters are tabulated in Table 1. C_6 and C_8 constants are taken from recent calculations performed by Proctor and

Stwalley.[7] The MMSV potential we obtained is plotted in Fig. 2, with the dotted portion of the curve indicating the region not accessed in our experiment.*

Other potential forms, such as a simple MSV, and the analytic potential proposed by Olson[5,3,2] were also tried. They however failed to yield very good agreement with the small angle data, Fig. 3. As we shall see later, discrepancies in this region cannot be compensated for by adjusting the imaginary part of the potential.

In the framework of semiclassical analysis, V_i, the complex component of the optical potential, plays no role in the trajectory of the particle which is solely controlled by V_0, the real part of the potential. This follows directly from the assumption that $V_0 >> V_i$, thus the semiclassical complex phase shift (for a potential $V_0 - iV_i$), namely,

$$\eta_\ell = \xi_\ell + i\,\zeta_\ell$$

$$= \hbar^{-1} \int_{Z_c}^{\infty + i\infty} \left[\left\{ 2\mu\,(E-V) - \frac{(\ell+\tfrac{1}{2})^2}{Z^2} \right\}^{\frac{1}{2}} - k \right] dZ - kZ_c$$

$$+ \frac{1}{2}\,\pi\,(\ell+\tfrac{1}{2})$$

$Z_c \equiv$ complex classical turning point

$$V = V_0 - iV_i \qquad (2)$$

can be expanded as a perturbation series, only the first term of which is retained, giving

$$\xi_\ell^0 = \hbar^{-1} \int_{r_c}^{\infty} \left[\left\{ 2\mu\,(E-V_0) - \frac{(\ell+\tfrac{1}{2})^2}{r^2} \right\}^{\frac{1}{2}} - k \right] dr - kr_c + \frac{1}{2}\,\pi\,(\ell+\tfrac{1}{2})$$

$$\zeta_\ell^0 = \hbar^{-1}\,(\tfrac{1}{2}\mu)^{\frac{1}{2}} \int_{r_c}^{\infty} \frac{V_i\,dr}{\left\{ E-V_0 - \left[\frac{\hbar^2(\ell+\tfrac{1}{2})^2}{2\mu r^2} \right] \right\}^{\frac{1}{2}}} \qquad (3)$$

*While this MMSV potential has about the same well depth as compared to the MSV potential previously reported by our group,[4] the location of its minimum has been shifted out. The slope of its repulsive wall is also less steep than before. It should be mentioned that the very recent calculation by Nakamura on $He(2^3S)+Ar$ was based on our old MSV potential.[13]

In this way, V_i serves only to characterize that confined region in which reaction can take place, and it is V_0 which determines how long the collision pair spends under the influence of V_i. Therefore, V_i, given as a function of interatomic distance, represents the extent of coupling between the discrete electronic state He^*-Ar and the He + Ar + e^- continuum. The coupling is expected to become stronger at shorter interatomic distances; in fact, an exponential behavior is generally considered as appropriate.[8,12]

In our previous report, the problem of parametrizing V_i was bypassed all together by parametrizing instead the opacity function which is related to V_i via

$$P_\ell = 1 - \exp(-4\zeta_\ell)$$

$$= 1 - \exp \int_{r_t}^{\infty} 4 \left(\frac{V_i(r)}{\hbar v_\ell(r)} \right) dr$$

where $v_\ell(r)$ is the radial velocity of the system moving in an effective potential $V_{eff}(r)$,

$$\left(\frac{\mu}{2}\right) v_\ell^2(r) = E - V_{eff}(r) = E - \left(\frac{\hbar^2 \ell(\ell+1)}{2\mu r^2} + V_0(r) \right) \qquad (5)$$

E is the collision energy, $V_0(r)$ is the real part of the potential, r_t is the classical turning point satisfying the condition

$$\left(\frac{\mu}{2}\right) v_\ell^2(r_t) = 0 = E - V_{eff}$$

While the opacity function is a more direct computational means to fit the data, its principle disadvantage lies in that the P_ℓ thus obtained seldom transcends in its application beyond the particular set of experimental data under consideration. On the other hand, general features in the optical potential can be more easily extended to understand

new data and to make predictions about other similar dynamical processes. We have therefore directed our pursuit towards finding the best V_i rather than P_ℓ. The parametric form for the optical potential we adopted was:

$$V_i(r) = \exp\left(-B(r-R_0)\right) \tag{6}$$

Of course, we recognize that the simple exponential form need not hold for very small r. For example, the calculations by Miller et al.for the system He(2S) +H yielded a V_i which levels off as $r \to 0$.[8]

Taking our best fit $V_0(r)$ and $V_i(r)$, we have calculated the total inelastic cross section as a function of relative velocity.

$$\sigma_{inel} = \pi k^{-2} \sum_{\ell} (2\ell+1)P_\ell \ . \tag{7}$$

The values we obtained are compared with the experimental results of Illenberger and Niehaus in Fig. 4.

DISCUSSION

A. Sources of Uncertainty

In fitting the data, we assumed that the real and imaginary components of the potential can be independently determined. This however is not strictly true if the available information is confined to only the differential cross section data. Specifically, there exists a trade-off relationship between the slope of the repulsive wall of V_0 determined by β_1 in Eq. (1), and the imaginary potential V_i. Thus one can have different combinations of β_1 and V_i all yielding the same fit to the differential cross section measured from 0° to 90° (lab.). However, if total ionization cross section measurements are made, especially as a function of kinetic energy, this ambiguity is removed. This is made apparent in Fig. 5 in which we show two such combinations of β_1 and V_i. We note while there is virtually no discernable difference in the calculated differential cross sections, the total cross section values obtained from them exhibit a marked dissimilarity.

In addition to the aforementioned indistinctness in the contributions of β_1 and V_i, $V_i(r)$ itself is the source of yet another

ambiguity. When V_i is changed to compensate for β_1 so that the calculated cross section remains the same, this can be accomplished in two ways. (a) $V_i(r)$ is uniformly increased or decreased by changing R_0 only; (b) the coefficient B in V_i is changed while keeping R_0 the same. The differential cross section measured at one kinetic energy is unable to distinguish which approach is more valid or realistic. Again, it is only by considering how these two different V_i's are reflected on the energy dependence of the total ionization cross section, one is able to secure the desirable confidence in a particular V_i. Of course, if differential cross section measurements are carried out over a wide range of energies, and if the oscillations at small angles are resolved for at least one energy (generally at low energy), then one can fairly uniquely determine both parts of the potential by imposing the principle of self-consistency without the need for total cross section data. This however is seldom realizable in practice. It is very difficult to get differential cross section information for the same broad range of energies as is routinely accomplished in total cross section measurements. The two sources of data therefore go hand in hand in establishing the most accurate potential.

Another assumption inherent in our analysis is that $V_i(r)$ is independent of the collision energy.* Thus we took for granted that the same optical potential should fit our data at 132 meV and 65 meV. V_i might have a weak and well-behaved energy dependence. We observed, for example, that the high energy data (132 meV) seemed to prefer a smaller V_i from that obtained at 65 meV. Also, with respect to the total ionization cross section, one can certainly fit more easily the data of Illenberger and Neihaus if V_i were made to decrease weakly as a function of energy. However, given the uncertainties in our high energy data, and the fact that we did not go high enough in energy, we cannot be very conclusive about this point. Work is currently underway to see if this is more prominently demonstrated in other systems.

*This assumption should be quite reasonable in the energy range experiments have been performed.

B. Validity of Semiclassical Approach

We have performed calculations to investigate the validity of the expressions (3) for the phase shift. Roberts and Ross[9] have already shown that, to a good approximation, the imaginary part of the phase shift can be calculated from Eq. (3) for a Lennard Jones or an exponential potential for a wide range of magnitudes of V_i. We found this to be the case with our MMSV potential also. However, significant deviation from the simple formula Eq. (3) for the real part of the phase shift was observed as V_i was increased. This deviation caused a large error in the differential elastic scattering cross section calculated from these phase shifts.

Formula (3) is based on the assumption that the real part of the phase shift does not change as the imaginary part of the potential is 'turned on'. We have investigated this assumption by comparing phase shifts calculated quantum mechanically for the potentials V_0 and $V_0 - iV_i$. We found a fairly simple relationship between the change in the real part of the phase shift and the magnitude of the opacity, Eq. (4). This relation, shown graphically in Fig. 6, is nearly independent of the size of V_i or the partial wave number. Thus if $\{\xi_\ell^\circ\}$ is the set of exact phase shifts for V_0 and $\{\xi_\ell + i\zeta_\ell\}$ those for $V_0 - iV_i$, we have plotted $|\xi_\ell - \xi_\ell^\circ|$ vs. $(1-e^{4\zeta_\ell})$. (Note: $\zeta_\ell \approx \zeta_\ell^0$). Figure 6 shows that as long as the opacity is smaller than about 0.9, the absolute error in ξ_ℓ is fairly small.

ξ_ℓ, however, is not a measurable quantity. In a practical calculation one normally calculates the differential cross section using the standard formula

$$\frac{d\sigma}{d\theta} = \sum_\ell (2\ell+1)\left[1-e^{2i[\xi_\ell - i\zeta_\ell]}\right] P_\ell(\cos\theta) \ . \qquad (8)$$

The overall reliability of Eq. (3) must be assessed by comparing the exact $(d\sigma/d\theta)$ (above) with that calculated using $\xi_\ell^\circ + i\zeta_\ell^\circ$. This is shown in Fig. 7. Using the best fit V_i, the quantum-mechanical and the approximate semiclassical results are essentially the same at 65 MeV. However, if V_i is increased by a factor of 5, the approximate semi-

classical analysis breaks down. Quantum mechanically, it is seen that as V_i is increased, only the large angle $(d\sigma/d\theta)$ is affected; $(d\sigma/d\theta)$ at small angles remains essentially unchanged. This is in accord with physical intuition.

When may Eq. (3) be safely employed? Although we know of no precise criteria, the following observations seem pertinent. For our optical Vi^{OPT}, all the opacities P_ℓ's have values ≤ 0.7. For 5 Vi^{OPT}, on the other hand, a sizable number of the partial waves with non-vanishing P_ℓ's have opacities exceeding 0.95. In fact, there are some 26 ℓ's, out of a total of 56 significant partial waves (with $P_\ell \geq 0.01$), for which there is approximately unit probability for ionization. Referring to Fig. (5a), we see that 5 Vi^{OPT} corresponds to a case where the magnitude of the imaginary part of the potential at the classical turning point becomes comparable to that of V_0, the real part of the potential. Under such circumstances, one does not expect the first order semiclassical approximation for the real part of the phase shifts to be reliable. If V_0 is predominently repulsive, a safe rule of thumb would be to carry out calculations for the desired V_i and also for twice that V_i. The two $\left(\frac{d\sigma}{d\theta}\right)$'s should be almost identical at small angles and only differ at large angles. If $\left(\frac{d\sigma}{d\theta}\right)$ changes significantly for small angles, Eq. (3) should not be used.

CONCLUSIONS

It is found that at low energies, for a given V_0, the total ionization cross section is much less sensitive to a particular V_i than at higher energies. Since the high energy data play such a vital role in determining V_i, it is important that there is no controversy in the measurements by different groups. This unfortunately is not the case. Pesnelli et al. and Illenberger and Niehaus have both investigated the energy dependence of the total ionization cross section. While their results agree at low energies, this congeniality fails to carry through to higher energies where radically different behaviors are observed by the two groups. We are decidedly biased in favoring Illenberger's data, which happen to agree with our own calculations. It would be most beneficial if another total ionization cross section measurement is made to arrest the existing uncertainty.

Other experiments which would lend additional confidence to our proposed V_0-iV_i should involve differential cross section measurements at many more different energies than what we have done. Higher velocities should be attempted, for as the collision energy goes up, the repulsive wall which the particle samples essentially rises infinitely fast, so that the classical turning point becomes fairly constant, and one ought then be able to observe the effect of V_i more vividly. It is only in this way can one establish how V_i behaves at small interatomic distances. V_0, on the other hand, is more keenly reflected in the differential cross section as the collision energy goes down. At low energies (such as that achieved by maintaining one of the beams at liquid nitrogen temperature), the oscillations at small angles can be more readily resolved, and they help to determine the interaction potential V_0 more precisely.

Up until now, theoretical effort on the He(2^3S)+Ar system has depended on model forms of the potentials V_0 and V_i, chosen to reproduce experimental results. Hickman and Morgner[11] have shown that once these curves are assumed, the quantum mechanical theory of Miller may be easily implemented. The development of a workable and efficient procedure for theoretically calculating V_0 and V_i is the only remaining obstacle to a more comprehensive understanding of Penning ionization from first principle. Present theoretical work is being directed along these lines.

FOOTNOTE AND REFERENCES

†This work is supported by the U. S. Energy Research and Development Administration.

‡Max-Planck Institut für Strömungsforschung, 3400 Göttingen, Böttingerstr. 6-8 West Germany.

1. A. Niehaus, Ber. Bunsenges, Phys. Chemie 77, 632 (1973), and also H. Hotop, Radiation Research 59, 379-404 (1974).
2. E. Illenberger and A. Niehaus, Z. Physik B 20, 33-41, (1975).
3. A. Pesnelle, G. Watel and C. Manus, J. Chem. Phys. 62, 3590-3600 (1975).
4. C. H. Chen, H. Haberland and Y. T. Lee, J. Chem. Phys. 61, 3095-3103 (1974).
5. R. E. Olson, Phys. Rev. A6, 1031-1036 (1972).
6. H. Haberland and C. Schmidt, private communicaiton, 1975.
7. T. R. Proctor and W. C. Stwalley, private communication, 1975.
8. W. H. Miller, C. A. Slocomb and H. F. Schaefer III, J. Chem. Phys. 56, 1347-1358 (1972).
9. R. E. Roberts and J. Ross, J. Chem. Phys. 52, 1464-1466 (1970).
10. J. T. Moseley, J. R. Peterson, D. C. Lorents and M. Hollstein, Phys. Rev. A6, 1025-1031 (1972).
11. A. P. Hickman and H. Morgner, J. Phys. B. 1975 (to be published).
12. H. Hotop and A. Niehaus, Z. Physik 238, 452-465 (1970).
13. N. Nakamura, J. Phys. B. 8, p. L489 (1975).

FIGURE CAPTIONS

Fig. 1a. Laboratory angular distribution of elastically scattered $He(2^3S)$ from Ar at 65 meV. Solid curve is the calculated differential cross section using the optical potential obtained in this work.

Fig. 1b. Laboratory angular distribution of elastically scattered $He(2^3S)$ from Ar at 132 meV. Solid line in the calculated theoretical curve.

Fig. 2. MMSV potential derived in this work, solid line. Dash-dot curve depicts the imaginary part of the optical potential. Dashed curve is the V_0 proposed by Olsen.[5]

Fig. 3. Comparison of the calculated differential cross sections using the optical potential derived in this work (solid line), and the analytic potential proposed by Olsen[5] with Illenberger's[2] coupling function (dashed line).

Fig. 4 Comparison of our calculated total ionization cross section as a function of relative velocity with Illenberger and Niehaus[2] experimental data (Δ).

Fig. 5a. The experimental differential cross section at 65 meV indiscriminately admits the two optical potentials above which are different only in the slope of their repulsive wall and their respective imaginary component. Solid line corresponds to the case of $\beta_1 = 5.2$, $V_i^{OPT} = \ell^{-5.2934(R-3.55)}$; dashed curves correspond to $\beta_1 = 4.5$ and $V_i = \ell^{-5.2934(R-3.35)}$. Dashed dot curve denotes $5\,V_i^{OPT}$.

Fig. 5b. The theoretical total ionization cross section vs. velocity using the two sets of $\{\beta_1, V_i\}$ in Fig. 5a. The solid line is that of $\beta_1 = 5.2$, $V_i = \ell^{-5.2934(R-3.55)}$, and is in good agreement with the data of Illenberger and Niehaus,[2] whereas the dashed curve is calculated from $\beta_1 = 4.5$, $V_i = \ell^{-5.2934\,(R-3.35)}$.

Fig. 6. Phase shifts ξ^0 are computed for the potential V_0 and compared with phase shifts $\xi+i\zeta$ for the cases of $V_0 - iV_i^{OPT}$, $V_0 - i(10Vi^{OPT})$ and $V_0 - i(100V_i^{OPT})$. The phase shifts are computed quantum mechanically by numerical integration (Numerov algorithm).

The calculations were done for several partial waves. We have plotted $\Delta\xi = |\xi_\ell - \xi_\ell^\circ|$ vs. the opacity, which is $(1-\exp(-4\zeta))$. For the first order semiclassical approximation, one assumes $\Delta\xi = 0$.

Fig. 7. Calculated differential cross sections, obtained by assuming a sharper resolution function for the detector, for the cases of V_i^{OPT} and $5\ V_i^{OPT}$. The curve for Vi^{OPT} is essentially identical to that obtained via a full quantum mechanical treatment. The curves for $5\ V_i^{OPT}$ are displaced to aid comparison.

Table 1. MMSV potential parameters

ϵ(kcal/mole)	0.1
r_m(Å)	5.5
β_1	5.2
β_2	5.7
C_6 (kcal/mole Å^6)	3048
C_8 (kcal/mole Å^8),	63678
b_1	0.75
b_2	1.119
b_3	-2.755
b_4	1.984
X_1	0
X_2	1.12
X_3	1.75

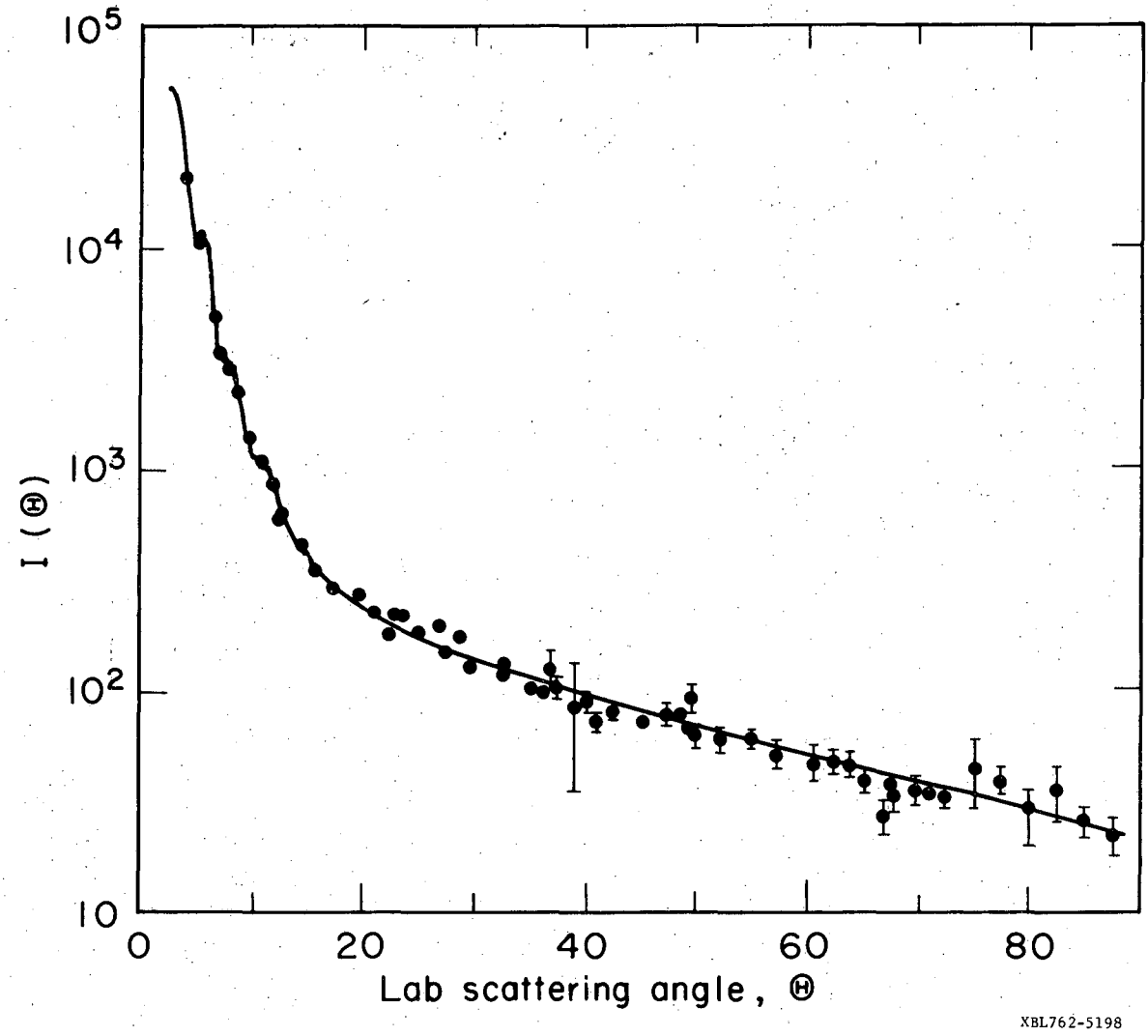

Fig. 1a

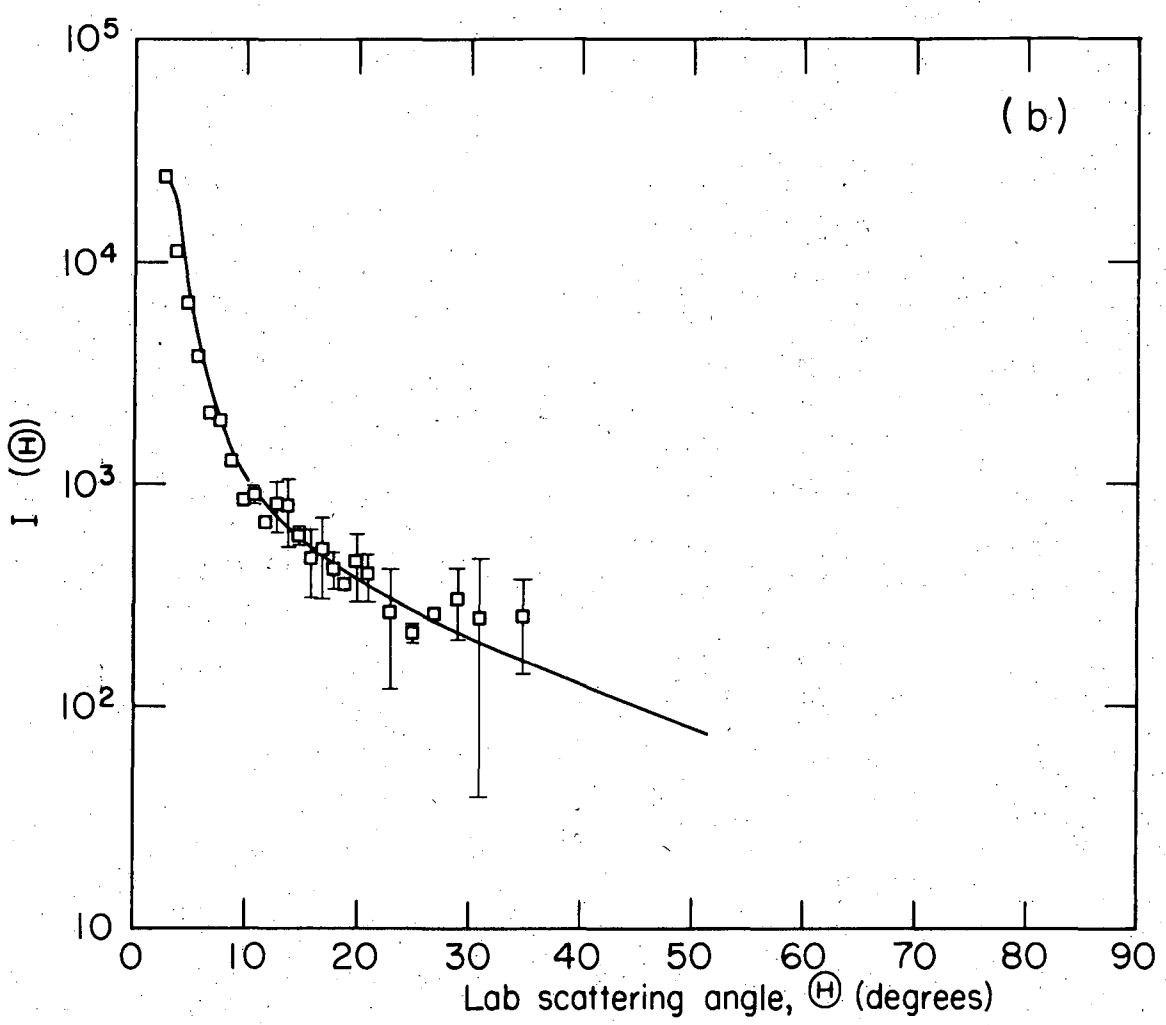

Fig. 1b

XBL 762-2206

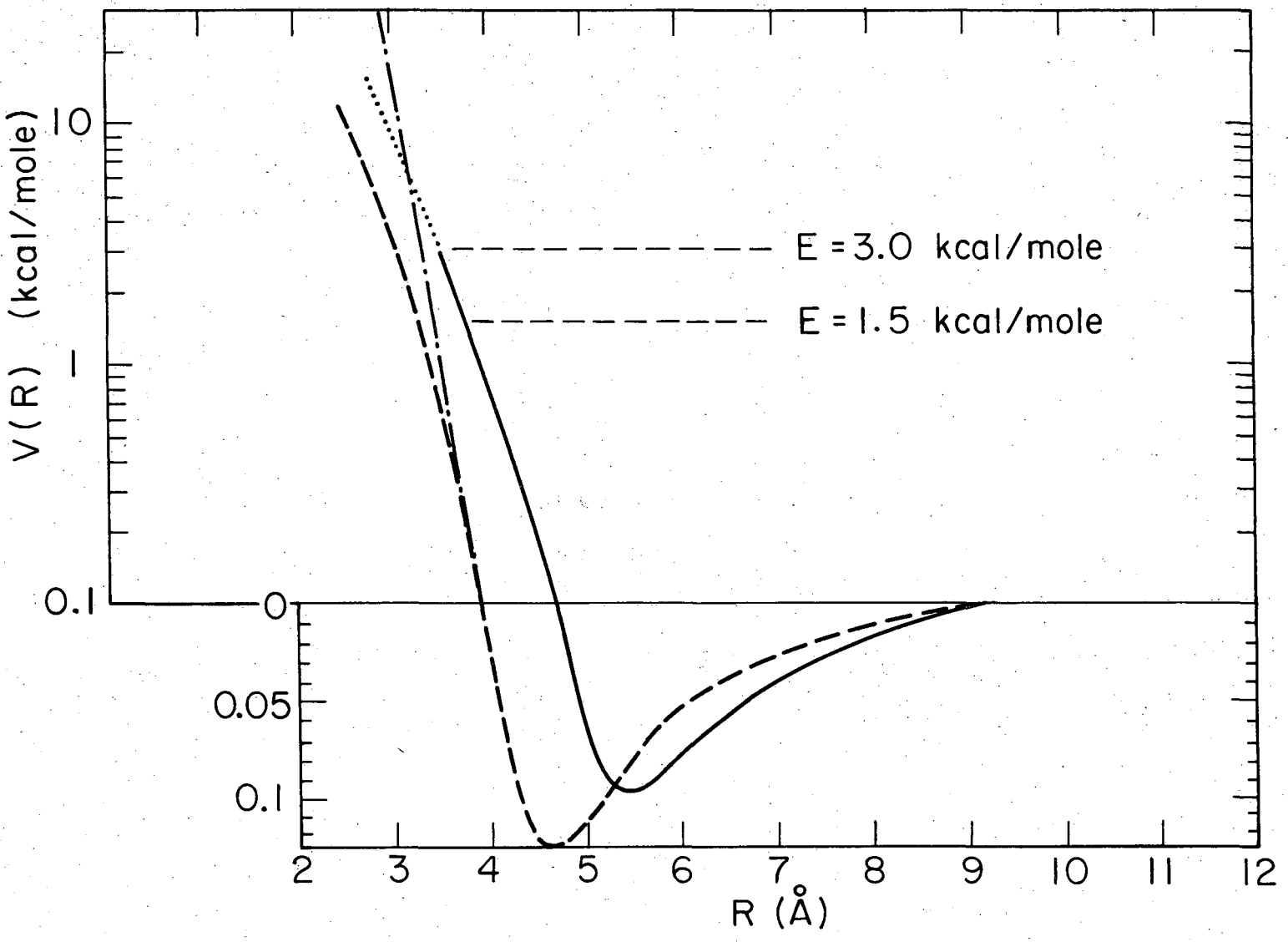

Fig. 2

XBL 762-2209

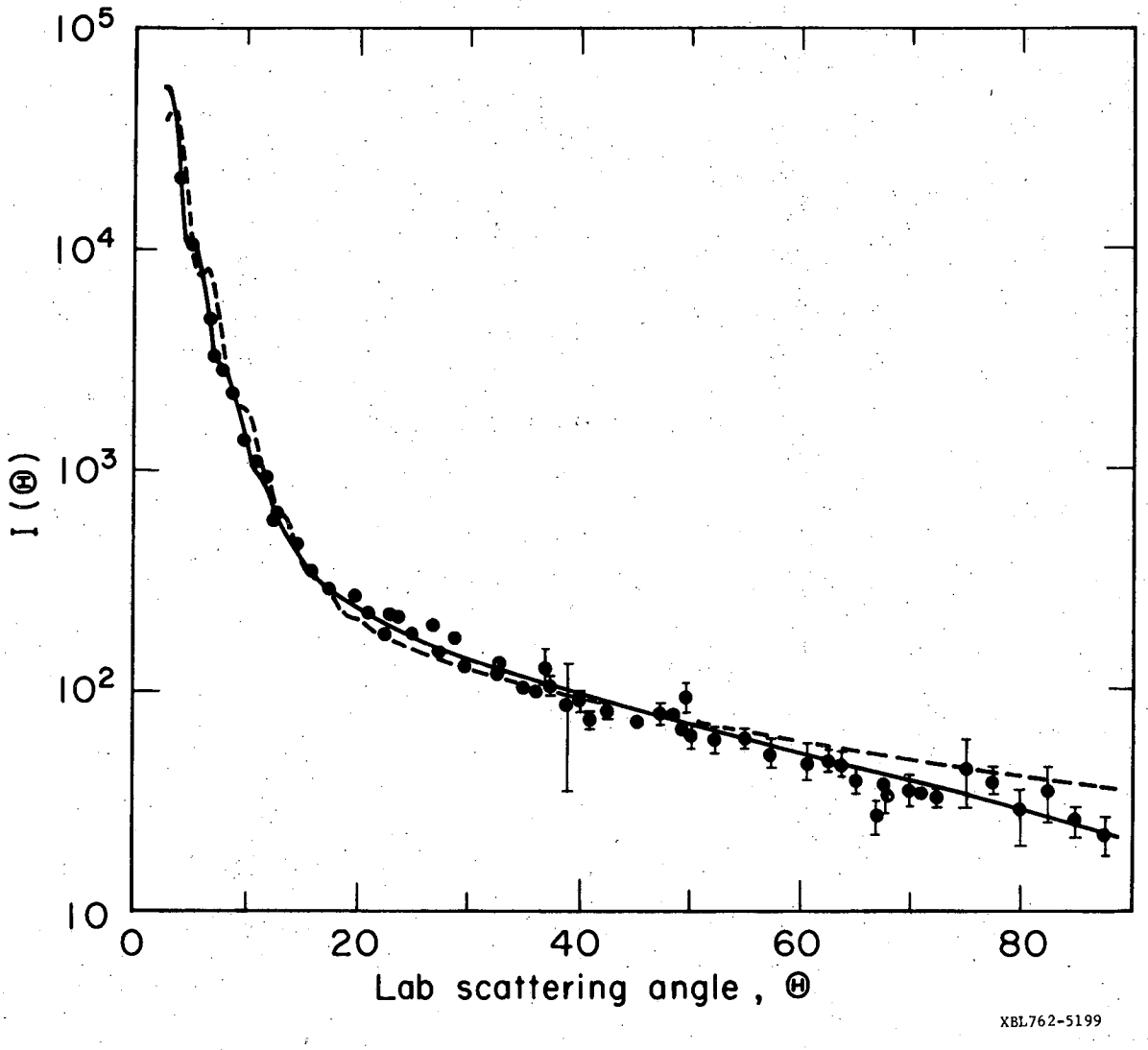
10^5
10^4
10^3
10^2
10
I (Θ)
0
20
40
60
80
Lab scattering angle , Θ
XBL762-5199

Fig. 3

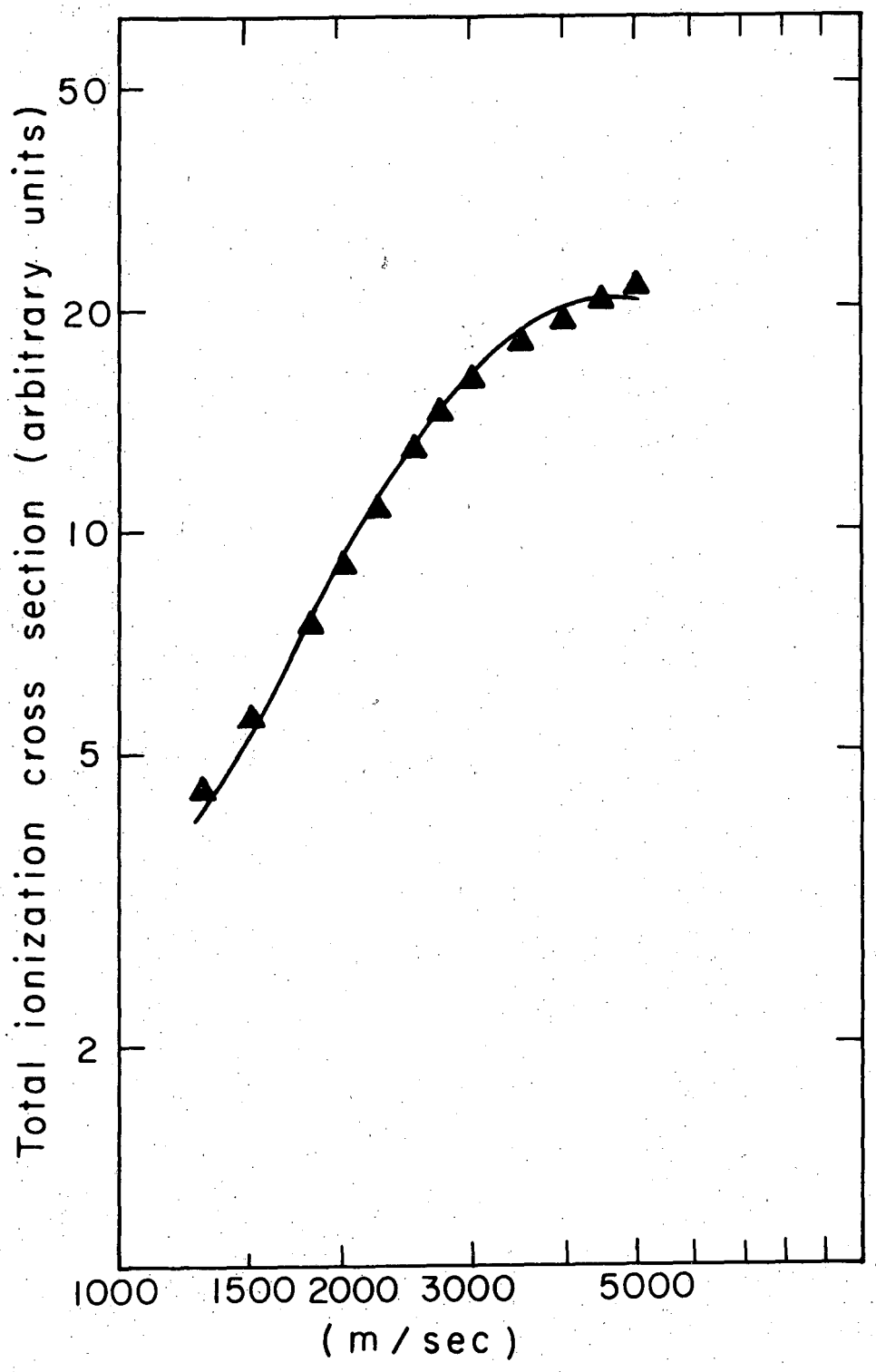

XBL 762-2201

Fig. 4

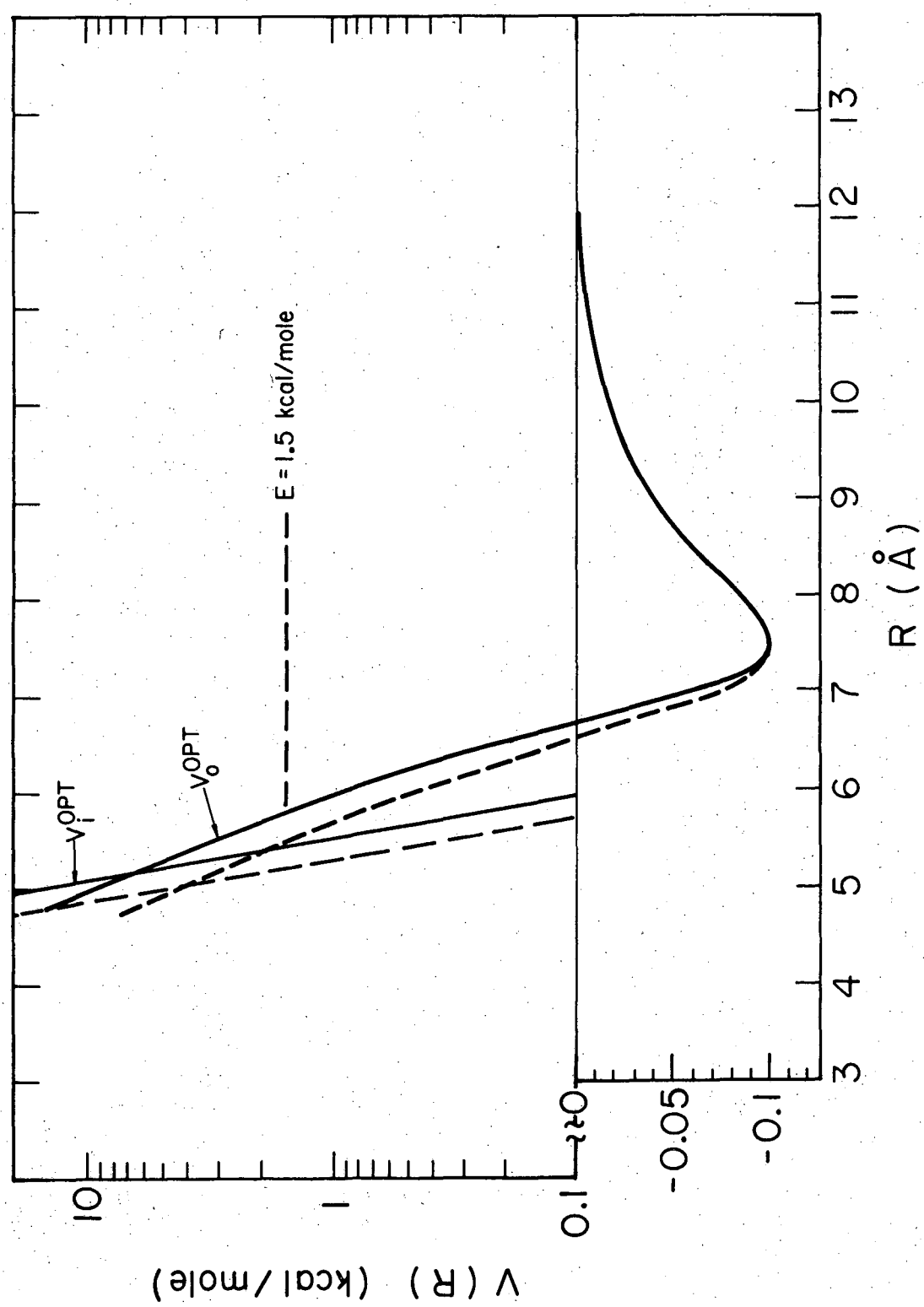

XBL 762-2210

Fig. 5a

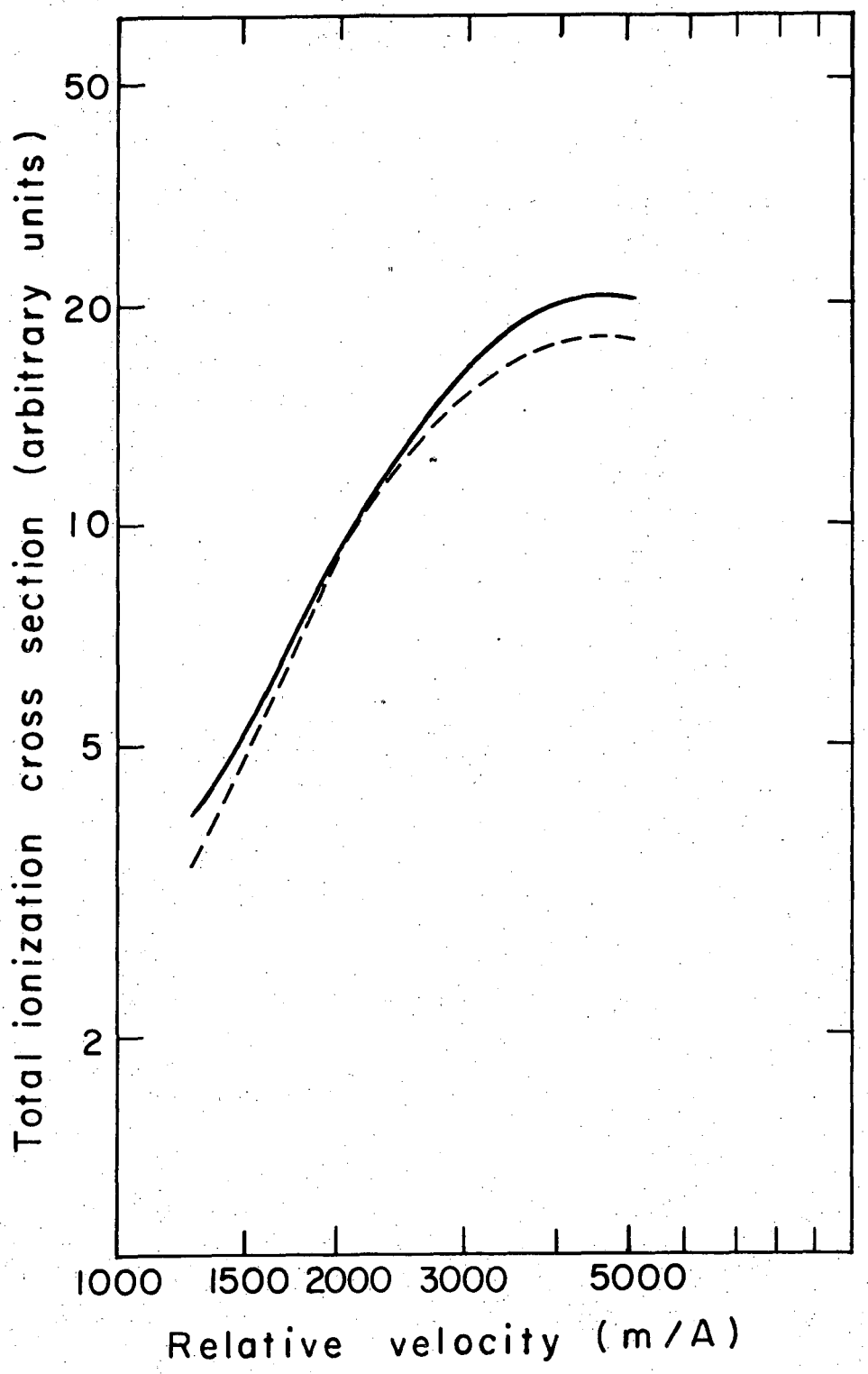

Fig. 5b

XBL 762-2202

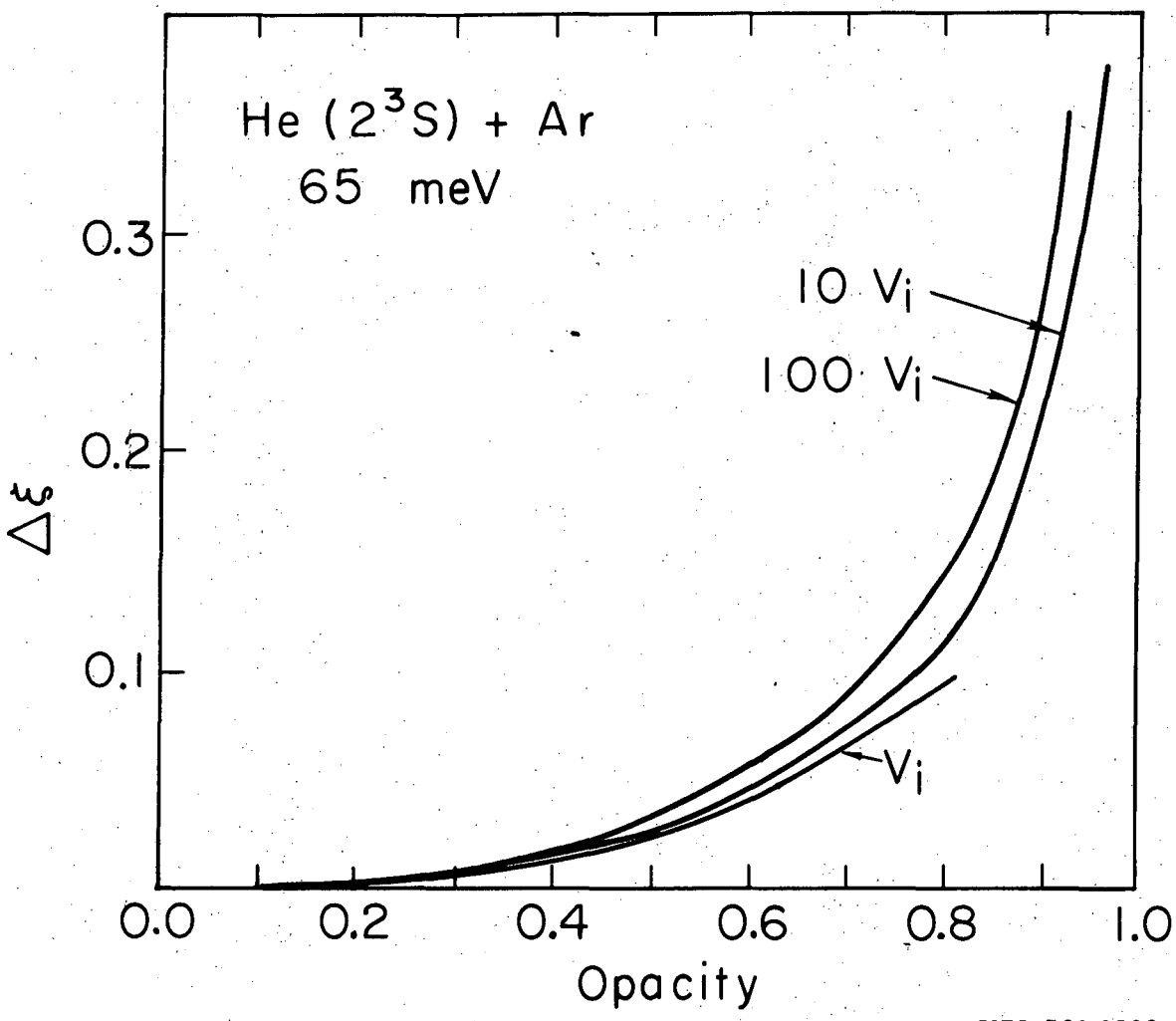

XBL 762-2203

Fig. 6

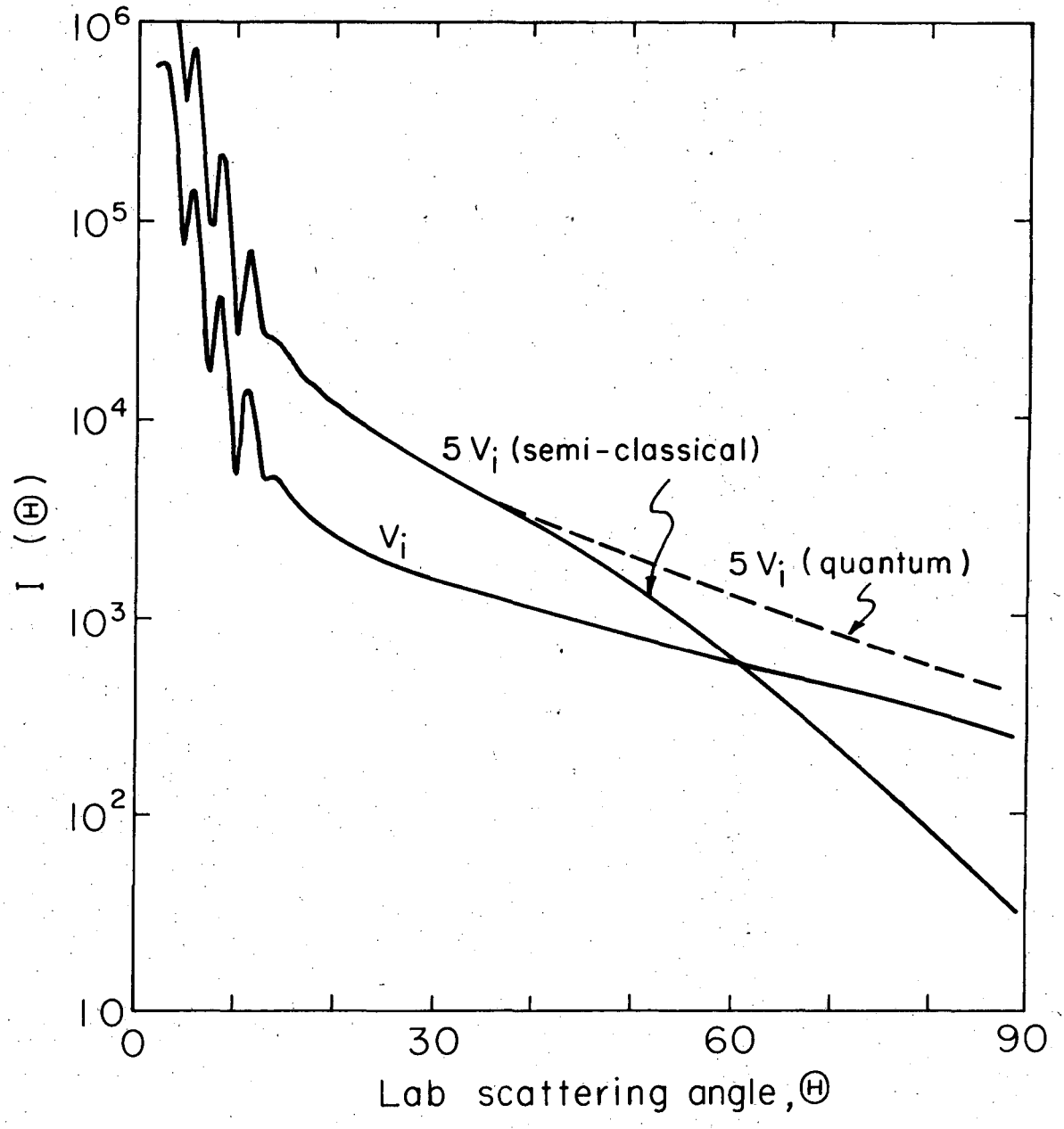

Fig. 7

XBL 762-2208

TECHNICAL INFORMATION DIVISION
LAWRENCE BERKELEY LABORATORY
UNIVERSITY OF CALIFORNIA
BERKELEY, CALIFORNIA 94720